

# Retinal Aquaporin-4 and Regulation of Water Inflow Into the Vitreous Body

Satoshi Ueki, Yuji Suzuki, and Hironaka Igarashi

Center for Integrated Human Brain Science, Brain Research Institute, Niigata University, Niigata, Japan

Correspondence: Satoshi Ueki, Center for Integrated Human Brain Science, Brain Research Institute, Niigata University, Asahimachi-dori 1-757, Chuo-ku, Niigata 951-8585, Japan; [sueki@bri.niigata-u.ac.jp](mailto:sueki@bri.niigata-u.ac.jp).

Received: October 2, 2020

Accepted: January 30, 2021

Published: February 18, 2021

Citation: Ueki S, Suzuki Y, Igarashi H. Retinal aquaporin-4 and regulation of water inflow into the vitreous body. *Invest Ophthalmol Vis Sci*. 2021;62(2):24. <https://doi.org/10.1167/iovs.62.2.24>

**PURPOSE.** Details of the posterior eye water dynamics are unclear. Aquaporin-4 (AQP4), a water channel, plays an important role in water dynamics in the central nervous system and is also present in the ocular tissue. The purpose of this study was to reveal the role of AQP4 in the water dynamics of the posterior eye using in vivo JJ vicinal coupling proton exchange (JJVCPE) magnetic resonance imaging (MRI) of AQP4 knockout (KO) mice and their wild-type littermates (controls).

**METHODS.** JJVCPE MRI of the eye was performed on five AQP4 KO mice and seven control mice. We assessed the normalized signal intensities of a region of interest (ROI) set in the vitreous body after  $H_2^{17}O$  administration. The results of the two groups were compared using a two-tailed Mann-Whitney *U* test.

**RESULTS.** A statistical analysis revealed that the normalized ROI signal intensities at the steady state were significantly lower ( $P = 0.010$ ,  $<0.05$ ) in the AQP4 KO mice (mean  $\pm$  SD,  $84.5\% \pm 2.7\%$ ) than the controls (mean  $\pm$  SD,  $88.8\% \pm 1.9\%$ ).

**CONCLUSIONS.** The present study using JJVCPE MRI of the eye demonstrated that retinal AQP4 has a potential role in the regulation of water inflow into the vitreous body. Absence of AQP4 in the KO mice probably induces lower water outflow from the vitreous body. Our results could help clarify the pathogenesis of various ocular diseases.

**Keywords:** aquaporin-4, magnetic resonance imaging, postiridial flow, Müller cells, knockout mice

Water dynamics in the eye are still poorly understood. In its anterior part, aqueous humor exits at the anterior chamber angle through the trabecular meshwork and uveoscleral routes.<sup>1</sup> However, water dynamics in the posterior eye have not been investigated in detail, despite indications of the existence of postiridial flow, that is, the flow of aqueous humor into the vitreous body, as previously shown by fluorescein distribution.<sup>2–4</sup> In the central nervous system (CNS), the role of aquaporin-4 (AQP4), one of the water channels, on water dynamics has received a lot of attention, and its mechanism has been elucidated.<sup>5,6</sup> AQP4 is also distributed abundantly in the ocular tissue (e.g., the ciliary epithelium and Müller cells of the retina).<sup>7</sup> Therefore, AQP4 has been suggested to be similarly involved in the water dynamics of the eye. JJ vicinal coupling proton exchange (JJVCPE) magnetic resonance imaging (MRI) has already been used to assess in vivo water dynamics in the mouse brain.<sup>8</sup> The  $H_2^{17}O$  influx, injected through the femoral vein, into the cerebrospinal fluid (CSF) can be observed as an  $H_2^{17}O$  dose-dependent signal reduction in T2-weighted magnetic resonance images. In the present study, we performed JJVCPE MRI of the eyes (JJVCPE MRI of the eye) of AQP4 knockout (KO) mice and their wild-type littermates (controls) to investigate the water dynamics of the posterior eye and reveal the role of AQP4 in it.

## METHODS

This study was approved and carried out in accordance with the animal research guidelines of the Institutional Review Board/Ethics Committee at Niigata University (Registration No. SA00642). This study was also performed to comply with the ARVO Statement for the Use of Animals in Ophthalmic and Vision Research. AQP4 KO mice and controls (both sexes; 11–18 weeks old;  $n = 5$  AQP4 KO mice;  $n = 7$  controls) underwent JJVCPE MRI of the eye. The generation of AQP4 KO mice has been described previously.<sup>9</sup> The mice resulted from homologous recombination using an embryonic stem cell line from the C57BL/6 strain.

JJVCPE MRI of the eyes were performed on a 15-cm bore, 7-T horizontal magnet (Magnex Scientific, Abingdon, UK) with a Varian Unity INOVA system (Varian, Palo Alto, CA, USA) equipped with an actively shielded gradient. The original JJVCPE MRI can assess in vivo water fluid dynamics in the mouse brain by setting a slab to include the CSF, the cortex, and the basal ganglia.<sup>8</sup> For the JJVCPE MRI of the eye, a 1-mm-thick 3-dimensional region of interest (ROI) was set to include a posterior portion of the left eye, containing the vitreous body (Fig. 1A). Adiabatic double spin-echo prepared rapid acquisition with refocused echoes was utilized with the following imaging parameters: 128  $\times$  128 matrix, 20  $\times$  20 mm<sup>2</sup> field of view, repetition time



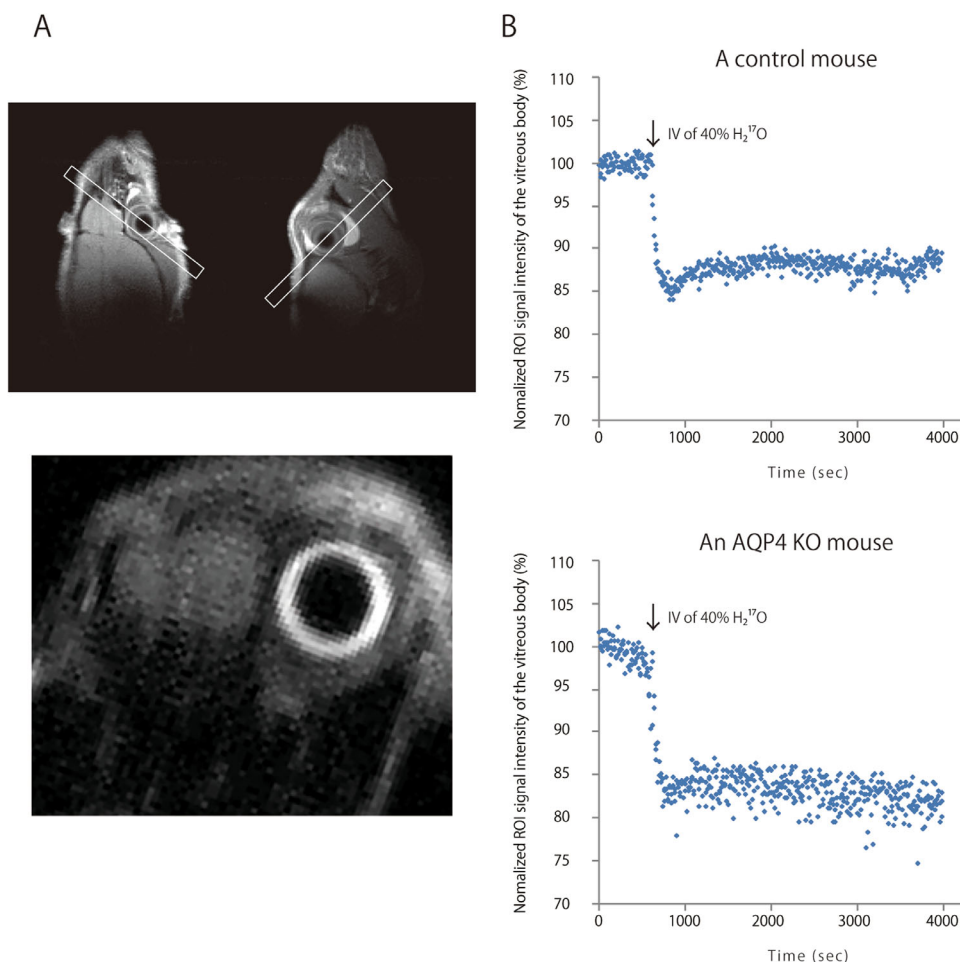


**FIGURE 1.** Result of a JJVCPE MRI of the eye in a control mouse and an AQP4 KO mouse. (A) A 1-mm-thick 3-dimensional (3-D) ROI was set to include a posterior portion of the left eye containing the vitreous body. The *upper part* shows a 3-D ROI (white rectangles) in coronal and sagittal T1-weighted images. The *lower part* shows the vitreous body of the left eye as donut shaped with high signal intensities in T2-weighted images by the sequences of adiabatic double spin-echo prepared rapid acquisition with refocused echoes. (B) The reduction of normalized ROI signal intensities, set to the vitreous body, after H<sub>2</sub><sup>17</sup>O administration is observed in a control mouse (*upper part*) and an AQP4 KO mouse (*lower part*) who underwent JJVCPE MRI of the eye. Normalized ROI signal intensities at steady state of a control mouse are greater than those of an AQP4 KO mouse.

2000 ms, echo train length 32, echo time (TE) for first echo 8.8 ms, echo spacing 5 ms, and effective TE 84.8 ms. The total scan time was 1 hour and 6 minutes for 500 scans per 8 seconds.

Before JJVCPE MRI of the eye, each mouse was anesthetized with inhaled isoflurane (0.01 mL/min), N<sub>2</sub>O (0.7 mL/min), and O<sub>2</sub> (0.3 mL/min), and PE10 tubing was inserted into the right femoral vein. Using 8-0 silk, a suture was carefully made between the left bulbar conjunctiva and the left upper palpebral conjunctiva to fixate the left eye. The left upper and lower eyelids were also sutured using 8-0 silk to prevent exposure of the cornea. During JJVCPE MRI of the eye, each mouse was anesthetized with intraperitoneal administration of urethane and dexmedetomidine hydrochloride (0.6 g/kg and 0.6 g/kg, respectively) and breathed spontaneously under inhaled N<sub>2</sub>O (0.7 mL/min) and O<sub>2</sub> (0.3 mL/min). Mice were positioned on their stomachs in a custom-made Plexiglas stereotaxic holder, and their heads were fixed in position by a tooth bar. Their rectal temperatures were main-

tained at  $37 \pm 0.5^{\circ}\text{C}$  using a custom-designed temperature control system. Normal saline (0.2 mL) containing 40% H<sub>2</sub><sup>17</sup>O was administered as an intravenous bolus injection 10 minutes after the first scan using an automatic injector at 0.04 mL/s through the PE10 tubing in the right femoral vein.

The images we obtained were analyzed using image processing software (MRVision, Winchester, MA, USA). The ROI was set to the vitreous body (Fig. 1A). Normalized ROI signal intensities, expressed as percentages against the average intensity of the identical pixels before H<sub>2</sub><sup>17</sup>O administration, were plotted against time (Fig. 1B). Normalized ROI signal intensity at steady state was determined by fitting their time course by a function previously described.<sup>8</sup> A two-tailed Mann-Whitney *U* test was used to compare the numerical data of the AQP4 KO and control mice. We selected the Mann-Whitney *U* test because of small sample size. Statistical analysis was done using GraphPad Prism 8 (GraphPad Software, La Jolla, CA, USA). A *P* value <0.05 was regarded as statistically significant.

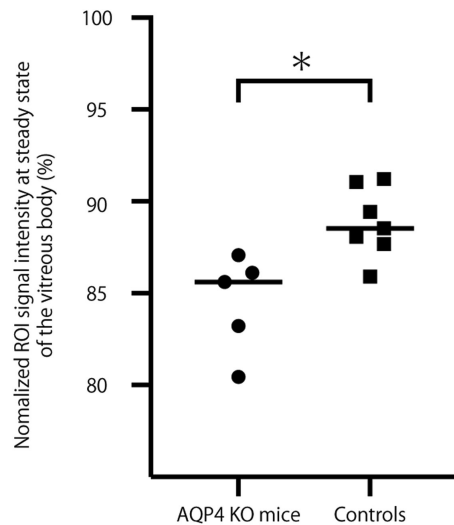


**FIGURE 2.** Normalized ROI signal intensities at steady state set to the vitreous body in AQP4 KO mice and controls. Normalized ROI signal intensities at steady state in the AQP4 KO mice are significantly lower than those of the controls as quantified by the two-tailed Mann-Whitney *U* test. Bars represent median values. \**P* < 0.05, Mann-Whitney *U* test.

## RESULTS

All 12 mice undergoing JJVCPE MRI of the eye showed a reduction in the normalized ROI signal intensity after  $H_2^{17}O$  administration. The representative results of an AQP4 KO and a control mouse are shown in Figure 1B. The signal intensity was reduced, and  $H_2^{17}O$  concentrations plateaued within 20 minutes.

Statistical analysis revealed that normalized ROI signal intensities at steady state were significantly lower ( $P = 0.010$ , <0.05) in the AQP4 KO mice ( $84.5\% \pm 2.7\%$ ) than in the controls ( $88.8\% \pm 1.9\%$ ) (Fig. 2).

## DISCUSSION

In the present study, JJVCPE MRI of the eye showed that water injected through the mouse femoral vein flowed relatively rapidly into the vitreous body of the mouse eye. Due to its nuclear magnetic resonance sensitivity,  $^{17}O$  interferes with the neighboring  $^1H$ s through a covalent bond in a phenomenon called JJ vicinal coupling. Accordingly, the influx of  $H_2^{17}O$  into ROIs in T2-weighted magnetic resonance images causes signal reduction. Based on the results of the studies on water dynamics in the posterior eye,<sup>2–4</sup> the water inflow into the vitreous body of the mouse eye detected in the present study probably observes a phenomenon called postiridial flow, an influx of aqueous humor into the vitreous body. In other words,  $H_2^{17}O$  injected through the mouse femoral vein is thought to flow into the vitreous body as a part of the aqueous humor produced at the ciliary epithelium because no other pathways of water entry into the vitreous body have been reported aside from postiridial flow.<sup>2–4</sup>

Furthermore, we revealed that normalized ROI signal intensities at steady state were significantly lower in the AQP4 KO mice than in the controls. The results indicate that water inflow into the vitreous body was higher in the AQP4 KO mice than in the controls and/or that water outflow

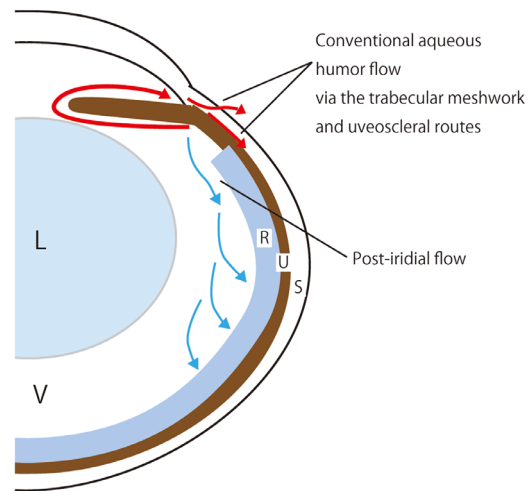


**FIGURE 3.** Schematic showing aqueous humor flows. A conventional flow is that where aqueous humor produced at the ciliary epithelium passes through the pupil to the anterior chamber angle (red arrow) via the trabecular meshwork and uveoscleral routes. On the other hand, a postiridial flow is that where aqueous humor produced at the ciliary epithelium passes through the vitreous body to the retina despite in an undetermined direction (blue arrows). L, lens; R, retina; S, sclera; U, uvea; V, vitreous body.

from the vitreous body was lower in the AQP4 KO mice than in the controls. Although the direction of the postiridial flow remains undetermined, it has been proposed that the aqueous humor produced at the ciliary epithelium passes through the vitreous body into the retina (Fig. 3).<sup>2–4</sup> In this route, AQP4 in the ciliary epithelium and in Müller cells of the retina<sup>7</sup> plays an important role. The impaired aqueous humor production at the ciliary epithelium in AQP4 KO mice induces lower water inflow into the vitreous body.<sup>10</sup> Our results propose an additional mechanism by which Müller cells in the retina would absorb water from the vitreous body through AQP4. In AQP4 KO mice, the capacity of Müller cells of absorbing water from the vitreous body is impaired, probably leading to lower water outflow from the vitreous body (Fig. 4).

In the retina, AQP4 is mainly distributed in Müller cells and has a prominent role in fluid homeostasis in the retina.<sup>11–13</sup> Immunohistochemical analyses have shown that AQP4 in Müller cells demonstrates colocalized distribution with Kir 4.1, which is a potassium channel.<sup>14</sup> Kir 4.1 has an important role in the spatial buffering of the retinal potassium, and owing to the colocalized distribution, AQP4 has a possibility of cooperating with Kir 4.1; however, it has been reported that AQP4 KO mice do not have impaired Kir 4.1 function.<sup>15</sup> AQP4 in Müller cells also demonstrates colocalized distribution with the transient receptor potential vanilloid 4 (TRPV4), which is a sensor for astroglial swelling.<sup>16</sup> TRPV4 should interact with AQP4 to sense glial swelling in Müller cells and astrocytes.<sup>17</sup>

In the CNS, AQP4 is mainly distributed in the foot processes of astrocytes,<sup>18</sup> and JJVCPE MRI has shown that water inflow into the CSF is reduced in AQP4 KO mice.<sup>8</sup> Nakada and Kwee<sup>6</sup> have proposed that water enters astrocytes through AQP4 and then moves into the pericapillary Virchow-Robin space. This proposal can be applied both to the water dynamics of the retina and that in the CNS. AQP4s in Müller cells are distributed in the end feet membranes

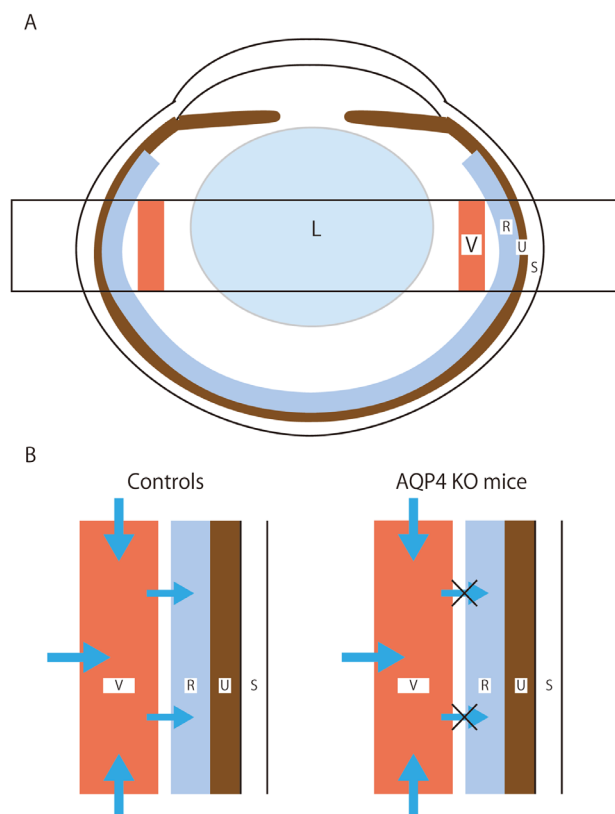


**FIGURE 4.** Presumed mechanisms explaining the results of the present study. **(A)** Schematic showing the anatomical relationships between the ocular tissue and a ROI set in the vitreous body. **(B)** Müller cells of the retina absorb water from the vitreous body through AQP4. Large blue arrows indicate inflow into the vitreous body. Small blue arrows indicate outflow from the vitreous body presumed by functionality of Müller cells' AQP4s. Compared to the controls (*left*), the water-absorbing function of Müller cells from the vitreous body diminishes and probably leads to lower water outflow from the vitreous body in the AQP4 KO mice (*right*).

facing the vitreous body and capillary endothelium.<sup>19</sup> We hypothesize that water absorbed through AQP4s in Müller cells would be released into the pericapillary Virchow-Robin space in the retina. A recent study has shown the pathway between the CSF and the pericapillary space in the optic nerve using fluorescent dextran.<sup>20</sup> The glymphatic pathway constituted by the perivascular flow is thought to be the clearance system of the interstitial solutes and proteins in the brain.<sup>5,6</sup> Daruich et al.<sup>13</sup> have proposed that the glymphatic pathway probably exists in the retina. We propose that the hypothesized water flow within the Müller cells, mentioned above, could drive the retinal "glymphatic pathway."

We investigated the water dynamics in the vitreous body by administration of sufficient dose of  $H_2^{17}O$  (approximately 2.7 mL/kg) to detect the signal changes in the vitreous body. Among the reports of MRI studies using  $H_2^{17}O$  as a non-radioactive trace,<sup>21–23</sup> Cheng et al.<sup>22</sup> demonstrated the signal changes in MRI of the rabbit eye after an intravenous  $H_2^{17}O$  injection, wherein the signal changes were not observed in the vitreous body and rapid signal changes were observed in the anterior chamber. Although our findings are different from those reported by them, this discrepancy may be due to the difference in the dose of  $H_2^{17}O$  (0.1 mL/kg in the study by Cheng et al.<sup>22</sup>) as they mentioned that sufficient

$H_2^{17}O$  should be loaded to visualize the signal changes in the vitreous body.

The present study utilizing JJVCPE MRI of the eye demonstrated that AQP4 in the retina has a potential role in the regulation of water inflow into the vitreous body via systemic circulation. Further investigation of the mechanism of aqueous humor in the posterior eye could contribute to elucidating the pathogenesis of various diseases (e.g., glaucoma and age-related macular degeneration) and the development of new treatments.

### Acknowledgments

The authors were motivated to reveal the role of AQP4 in water dynamics of the posterior eye after the review published by Nakada et al.<sup>5</sup> Although Professor Nakada passed away in July 2018, his review contributed a lot to this study.

Supported by JSPS KAKENHI, Grant 18K09441.

Disclosure: S. Ueki, None; Y. Suzuki, None; H. Igarashi, None

### References

- Gabelt BT, Kaufman PL. Production and flow of aqueous humor. In: Levin LA, Nilsson SFE, Ver Hoeve J, Wu S, Kaufman P, Alm A, eds. *Adler's Physiology of the Eye*. 11th ed. Amsterdam, Netherlands: Elsevier; 2011:274–307.
- Araie M, Maurice DM. The loss of fluorescein, fluorescein glucuronide and fluorescein isothiocyanate dextran from the vitreous by the anterior and retinal pathways. *Exp Eye Res*. 1991;52:27–39.
- Araie M, Sugiura Y, Sakurai M, Oshika T. Effect of systemic acetazolamide on the fluid movement across the aqueous-vitreous interface. *Exp Eye Res*. 1991;53:285–293.
- Tsuboi S. Measurement of the volume flow and hydraulic conductivity across the isolated dog retinal pigment epithelium. *Invest Ophthalmol Vis Sci*. 1987;28:1776–1782.
- Nakada T, Kwee IL, Igarashi H, Suzuki Y. Aquaporin-4 functionality and Virchow-Robin space water dynamics: physiological model for neurovascular coupling and glymphatic flow. *Int J Mol Sci*. 2017;18:1798.
- Nakada T, Kwee IL. Fluid dynamics inside the brain barrier: current concept of interstitial flow, glymphatic flow, and cerebrospinal fluid circulation in the brain *Neuroscientist*. 2019;25:155–166.
- Verkman AS, Ruiz-Ederra J, Levin MH. Functions of aquaporins in the eye. *Prog Retin Eye Res*. 2008;27:420–433.
- Igarashi H, Tsujita M, Kwee IL, Nakada T. Water influx into cerebrospinal fluid is primarily controlled by aquaporin-4, not by aquaporin-1:  $^{17}O$  JJVCPE MRI study in knockout mice. *Neuroreport*. 2014;25:39–43.
- Kitaura H, Tsujita M, Huber VJ, et al. Activity-dependent glial swelling is impaired in aquaporin-4 knockout mice. *Neurosci Res*. 2009;64:208–212.
- Zhang D, Vetrivel L, Verkman AS. Aquaporin deletion in mice reduces intraocular pressure and aqueous fluid production. *J Gen Physiol*. 2002;119:561–569.
- Bringmann A, Pannicke T, Grosche J, et al. Müller cells in the healthy and diseased retina. *Prog Retin Eye Res*. 2006;25:397–424.
- Goodyear MJ, Crewther SG, Junghans BM. A role for aquaporin-4 in fluid regulation in the inner retina. *Vis Neurosci*. 2009;26:159–165.
- Daruich A, Matet A, Moulin A, et al. Mechanisms of macular edema: beyond the surface. *Prog Retin Eye Res*. 2018;63:20–68.



14. Schey KL, Wang Z, Wenke JL, Qi Y. Aquaporins in the eye: expression, function, and roles in ocular disease. *Biochim Biophys Acta*. 2014;1840:1513–1523.
15. Ruiz-Ederra J, Zhang H, Verkman AS. Evidence against functional interaction between aquaporin-4 water channels and Kir4.1 potassium channels in retinal Müller cells. *J Biol Chem*. 2007;282:21866–21872.
16. Jo AO, Ryskamp DA, Phuong TTT, et al. TRPV4 and AQP4 channels synergistically regulate cell volume and calcium homeostasis in retinal Müller glia. *J Neurosci*. 2015;35:13525–13537.
17. Benfenati V, Caprini M, Dovizio M, et al. An aquaporin-4/transient receptor potential vanilloid 4 (AQP4/TRPV4) complex is essential for cell-volume control in astrocytes. *Proc Natl Acad Sci USA*. 2011;108:2563–2568.
18. Nagelhus EA, Ottersen OP. Physiological roles of aquaporin-4 in brain. *Physiol Rev*. 2013;93:1543–1562.
19. Nagelhus EA, Horio Y, Inanobe A, et al. Immunogold evidence suggests that coupling of K<sup>+</sup> siphoning and water transport in rat retinal Müller cells is mediated by a coenrichment of Kir4.1 and AQP4 in specific membrane domains. *Glia*. 1999;26:47–54.
20. Mathieu E, Gupta N, Ahari A, Zhou X, Hanna J, Yücel YH. Evidence for cerebrospinal fluid entry into the optic nerve via a glymphatic pathway. *Invest Ophthalmol Vis Sci*. 2017;58:4784–4791.
21. Kwong KK, Hopkins AL, Belliveau JW, et al. Proton NMR imaging of cerebral blood flow using H<sub>2</sub>(17)O. *Magn Reson Med*. 1991;22:154–158.
22. Cheng HM, Kwong KK, Xiong J, Woods BT. Visualization of water movement in the living rabbit eye. *Graefes Arch Clin Exp Ophthalmol*. 1992;30:62–65.
23. Ronen I, Merkle H, Ugurbil K, Navon G. Imaging of H<sub>2</sub><sup>17</sup>O distribution in the brain of a live rat by using proton-detected <sup>17</sup>O MRI. *Proc Natl Acad Sci USA*. 1998;95:12934–12939.